Time-frequency analysis of wakes produced by turning ships

Ravindra Pethiyagoda, **Timothy J. Moroney**, **Scott W. McCue**

School of Mathematical Sciences, Queensland University of Technology, Brisbane QLD 4001, Australia

1. Introduction

The use of time-frequency analysis to study ship wakes is the subject of much interest [1, 3, 8, 9, 10, 11, 12]. In particular, the use of short-time Fourier transforms to decompose a ship's wake into a time-frequency heat-map known as a spectrogram has seen some success in identifying different features of ship wakes (eg., their transverse and divergent waves) observed in real shipping channels and in experimental towing tanks [3, 8, 11]. A spectrogram has the advantage that it only requires information from the surface elevation at one physical location, necessitating a single stationary sensor [3, 5]. The practical applications of accurately identifying properties of a ship wake from such easily accessible data range from environmental conservation (eg. determining if a group of strong waves that negatively effect a coastline originated from a ship [10]) to security (eg. identifying the presence of unmonitored ships).

Recently, we studied spectrograms of steady ship wakes [6, 8]. Using linear water wave theory, we showed that regions of the highest colour intensity on the spectrograms followed a curve referred to as the linear dispersion curve. In [6], for an infinitely deep fluid, we also used numerical solutions to the fully nonlinear problem (computed with the scheme outlined in [7]) to help predict the location of higher order modes. In the present study, we shall extend the linear framework to apply for a ship travelling along a circular path with constant angular velocity. In Section 2 we use geometric arguments and the linear dispersion relation to derive a relationship between the frequency of the waves travelling at the group velocity and the time they reach a fixed sensor (this is the dispersion curve). Then, in Section 3, we propose a very simple model for a ship which involves a pressure distribution applied to the surface. Assuming this disturbance starts moving from a point in space and then travels in a circular path, we use Fourier transforms to derive an exact solution for the wave signal. With this signal, we compute spectrograms and discuss the results briefly in Section 4.

2. Linear dispersion curve

Suppose we have a disturbance (a ship, say) travelling along a circular path with constant tangential speed U. We consider the non-dimensional problem by scaling speeds by U, lengths by U^2/g, and time by U/g, where g is acceleration due to gravity. The path of the ship relative to the sensor is given by

$$\mathbf{X}(t) = (x_c + R\cos(t/R), R\sin(t/R)), \qquad \mathbf{U}(t) = (-\sin(t/R), \cos(t/R)), \tag{1}$$

where $\mathbf{U}(t) = \mathbf{X}'(t)$ is the velocity, x_c is the centre of the turning circle, and R is the circle radius. Assuming an infinitely deep fluid, the dispersion relation, phase and group velocities are

$$\omega = \sqrt{k}, \qquad c_p = \frac{1}{\sqrt{k}}, \qquad c_g = \frac{1}{2\sqrt{k}} = \frac{c_p}{2}, \tag{2}$$

respectively, where ω is the wave frequency, and k is the wavenumber.

To construct the linear dispersion curve (t, ω), we consider the following properties. First, as the ship moves it will generate waves that propagate towards the sensor with phase velocity given by the Doppler shifted dispersion relation

$$c_p = \frac{1}{\sqrt{k}} = \cos\psi = \frac{-\mathbf{X}\cdot\mathbf{U}}{r}, \tag{3}$$

where ψ is the angle between the sailing line and the sensor, and $r(t) = |\mathbf{X}(t)|$ is the radial distance from the ship to the sensor as illustrated in Figure 1. The second property is that the dispersive wave packet detected by the sensor travels at the group velocity. Combining these properties with the dispersion relation (2), we find

$$(t, \omega) = \left(\tau + \frac{r(\tau)}{c_g(\tau)}, \sqrt{k(\tau)}\right), \tag{4}$$

where $k(\tau)$ can be determined through (3), and τ is the time the wave packet is generated. For our disturbance travelling in the circular path (1), this dispersion curve (4) simplifies to

$$(t, \omega) = \left(\tau + 2\frac{x_c^2 + R^2 + 2x_cR\cos\tau/R}{x_cR\sin\tau/R}, \frac{\sqrt{x_c^2 + R^2 + 2x_cR\cos\tau/R}}{x_cR\sin\tau/R}\right).$$

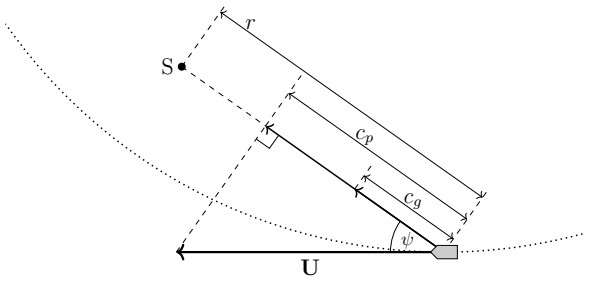

Figure 1: A schematic of a ship (grey object) moving with velocity $\mathbf{U}$ near a wave sensor S. r is the radial distance between the ship and the sensor and ψ is the angle between the sailing line and the sensor. The ship will generate waves travelling with phase velocity, c_p, and group velocity, c_g. The dotted curve is a portion of the circular path taken by the ship.

3. Linear wave signal

Consider an axisymmetric pressure distribution applied to the surface of the fluid travelling along the path (1). To derive the wave signal produced by this disturbance, we first consider the surface elevation $\zeta_p(r,t)$ produced by a pulse of this pressure over $\delta(t)$ (the Dirac delta function), which we shall later integrate in time over the path. The governing equations for this part of the solution are [2]

$$\frac{\mathrm{d}^2\tilde{\zeta}_p}{\mathrm{d}t^2} + k\tilde{\zeta}_p = -k\delta(t)\tilde{p}(k), \quad \tilde{\zeta}_p|_{t=0} = 0, \quad \frac{\mathrm{d}\tilde{\zeta}_p}{\mathrm{d}t}\Big|_{t=0} = 0, \tag{5}$$

where k is the wavenumber, $\tilde{\zeta}_p(k,t)$ is the Fourier transform of $\zeta_p(r,t)$, $\tilde{p}(k) = \epsilon\exp(-k^2/4\pi^2F^4)$ is the Fourier transform of the pressure distribution, $F = U/\sqrt{gL}$ is the Froude number, and L is a length-scale related to the pressure distribution. Solving (5) and inverting the Fourier transform gives

$$\zeta_p(r,t) = -\frac{1}{2\pi}\int_0^\infty k^{3/2}\tilde{p}(k)\sin\left(\sqrt{k}t\right)J_0(kr)\,\mathrm{d}k,$$

where $J_0(x)$ is the Bessel function of the first kind of order zero and r is the radial distance from the centre of the disturbance.

In order to smooth the signal at $t = 0$, we suppose the axisymmetric pressure distribution had been fixed in place and applied to the surface for all time $t < 0$. The equations for this initial disturbance are

$$\frac{\mathrm{d}^2\tilde{\zeta}_i}{\mathrm{d}t^2} + k\tilde{\zeta}_i = 0, \quad \tilde{\zeta}_i|_{t=0} = -\tilde{p}(k), \quad \frac{\mathrm{d}\tilde{\zeta}_i}{\mathrm{d}t}\Big|_{t=0} = 0, \tag{6}$$

where $\tilde{\zeta}_i(k,t)$ is the Fourier transform of the surface elevation due to this initial disturbance. Solving (6) and inverting the Fourier transform gives

$$\zeta_i(r,t) = -\frac{1}{2\pi}\int_0^\infty k\tilde{p}(k)\cos\left(\sqrt{k}t\right)J_0(kr)\,\mathrm{d}k.$$

We can now construct the complete wave signal as the superposition of the initial disturbance and the pressure pulse integrated along the ship's path $\mathbf{X}(t)$, giving

$$s(t) = \zeta_i(r(0),t) + \int_0^t \zeta_p(r(\tau),t-\tau)\,\mathrm{d}\tau,$$

where we recall from (1) that $r(t) = |\mathbf{X}(t)|$.

The spectrogram for the signal $s(t)$ is given by the square magnitude of the short-time Fourier Transform

$$S(t,\omega) = \left|\int_{-\infty}^{\infty} h(\tau - t)s(t)\mathrm{e}^{-\mathrm{i}\omega\tau}\,\mathrm{d}\tau\right|^2,$$

where the window function, $h(t)$, is an even function with compact support (we use the Blackman-Harris 92 dB window function [4]). All spectrograms are plotted on the scaled axis $((t-t_c)/r_{\min},\omega)$, where t_c and $r_{\min}$ are the time and distance for when the ship is closest to the sensor, that is $\min(r(t)) = r(t_c) = r_{\min}$. For the ship path given by (1), $t_c = \pi R$ and $r_{\min} = |x_c - R|$.

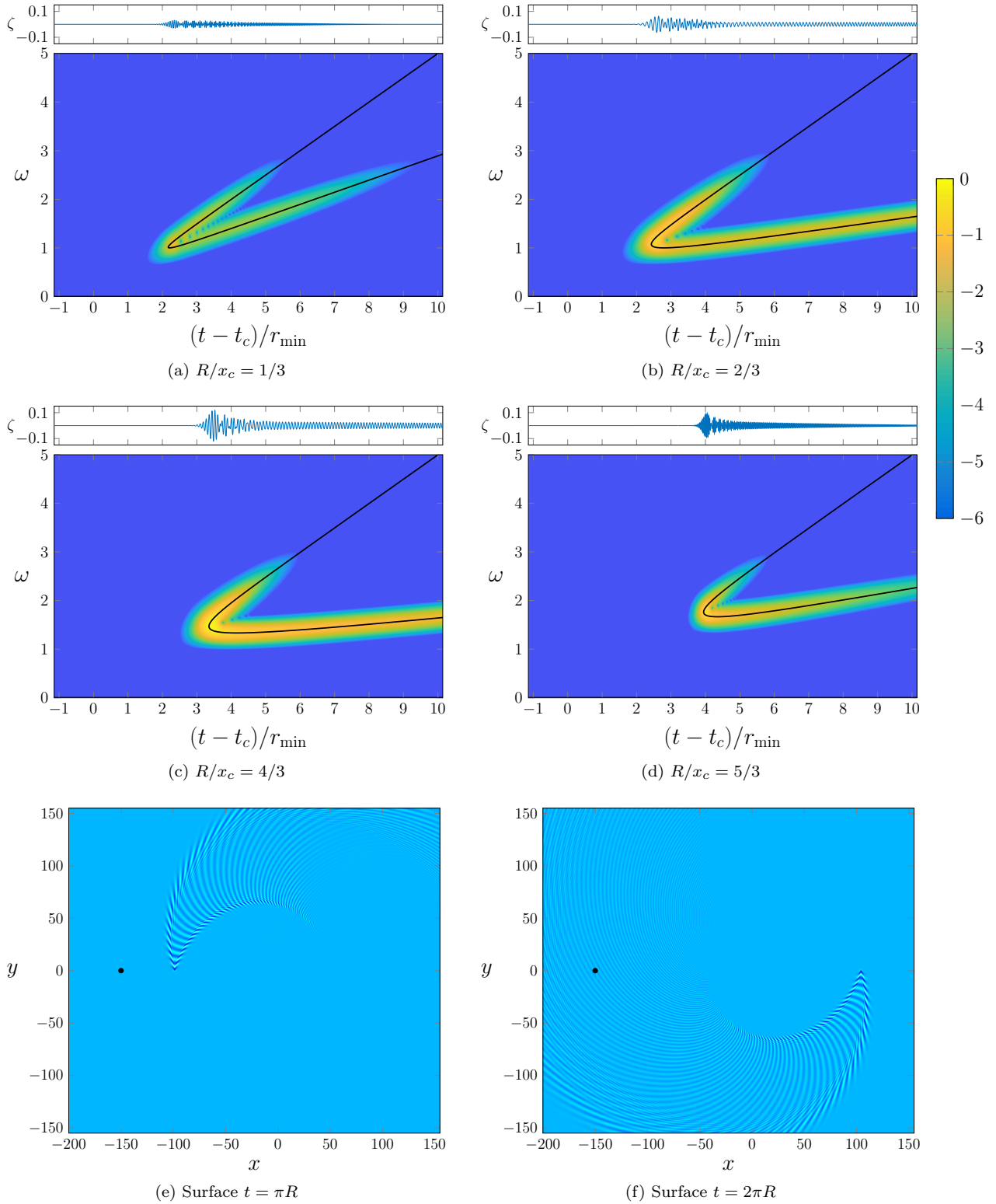

(a) $R/x_c = 1/3$

(b) $R/x_c = 2/3$

(c) $R/x_c = 4/3$

(d) $R/x_c = 5/3$

(e) Surface $t = \pi R$

(f) Surface $t = 2\pi R$

Figure 2: Spectrograms computed for a pressure distribution travelling in a circle with unit tangential velocity positioned either (a)-(b) outside or (c)-(d) inside the turning circle. The circle centre and Froude number are $x_c = 150$ and $F = 0.7$, respectively. The linear dispersion (black) curve is overlaid. (e)-(f) shows the wave pattern corresponding to the spectrogram in part (b) at two different times, $t = \pi R$, $2\pi R$. The black dot represents the location of the sensor.

4. Results and discussion

Figure 2 presents spectrograms for a turning ship where the sensor is (a)-(b) outside or (c)-(d) inside the circular path, with the linear dispersion (black) curve overlaid. We see very strong agreement between the regions of high colour intensity in the spectrogram and the linear dispersion curve. Note that the colour intensity appears higher in parts (b) and (c) as the ship is closer to the sensor for those two examples (the minimum distance is 50 in both cases), when compared to (a) and (d) (here the minimum distance is 100 for these two examples). Note also that these four spectrograms are all drawn for a single Froude number, $F = 0.7$; for different Froude numbers (not shown here), the highest intensity regions shift to other parts of the dispersion curve (see [6] for an analogous discussion for steady wakes).

In all the examples in Figure 2, the linear dispersion curve is comprised of two branches with the upper branch approaching the line $\omega = (t - t_c)/2r_{\min}$ and the lower branch approaching the line $\omega = t/2r(0)$ as $t \to \infty$. The gradients of the asymptotic behaviour of the branches can be used to directly estimate the smallest distance the ship is from the sensor $r_{\min}$ (upper branch) and the starting distance $r(0)$ (lower branch). Additionally, for $R/x_c < 1$ the linear dispersion curve has a minimum frequency of $\omega = 1$ produced when the ship is moving directly towards the sensor. Therefore, if it is known that the sensor lies outside the ships turning circle, the minimum frequency can be used to estimate the speed of the ship.

If we were to classify transverse waves by $\psi < \tan^{-1}(1/\sqrt{2})$ and divergent waves by $\psi > \tan^{-1}(1/\sqrt{2})$ (where ψ is shown in Figure 1), which is done routinely for ships moving steadily in one direction, the tails of both branches are formed by divergent waves and the region near the fold is formed by transverse waves. This property is very different from that for a ship travelling in a straight line, for which the upper branch corresponds to the divergent waves and the lower branch corresponds to the transverse waves. This apparent contradiction is worth exploring in more detail.

For completeness, in Figure 2(e)-(f) we show wave patterns drawn for the same parameters as those corresponding to the spectrogram in Figure 2(b) (here the sensor is outside of the circular path). The wave patterns are shown for two different times, namely $t = \pi R$ (when the disturbance is closest to the sensor) and $t = 2\pi R$ (when the disturbance is furthest away from the sensor). One interesting feature of these patterns is the way in which the familiar divergent and transverse waves are distorted and interfering in certain regions of the wake (see near $(x, y) = (-150, -100)$ in (f), for example).

In summary, we have extended the framework for computing spectrograms of steady ship wakes to apply for disturbances travelling in a circular path with constant angular velocity. This is a significant step towards a more general study in which the ship can travel on any path. Future work involves better models for ships, a more general bathymetry, experimental validation, and further analysing the inverse problem of determining properties of a ship wake given its spectrogram.

Acknowledgements

This work is supported by the Australian Research Council via DP180103260.

References

[1] E. D. Brown, S. B. Buchsbaum, R. E. Hall, J. P. Penhune, K. F. Schmitt, K. M. Watson, and D. C. Wyatt. Observations of a nonlinear solitary wave packet in the Kelvin wake of a ship. *J. Fluid Mech.*, 204:263–293, 1989.

[2] A. D. Chepelianskii, F. Chevy, and E. Raphaël. Capillary-gravity waves generated by a slow moving object. *Phys. Rev. Lett.*, 100:074504, 2008.

[3] I. Didenkulova, A. Sheremet, T. Torsvik, and T. Soomere. Characteristic properties of different vessel wake signals. *J. Coast. Res.*, SI 65:213–218, 2013.

[4] F. J. Harris. On the use of windows for harmonic analysis with the discrete Fourier transform. *Proc. IEEE*, 66:51–83, 1978.

[5] K. Parnell, N. Delpeche, I. Didenkulova, T. Dolphin, A. Erm, A. Kask, L. Kelpšaite, D. Kurennoy, E. Quak, and A. Räämet. Far-field vessel wakes in Tallinn Bay. *Est. J. Eng.*, 14:273–302, 2008.

[6] R. Pethiyagoda, S. W. McCue, and T. J. Moroney. Spectrograms of ship wakes: identifying linear and nonlinear wave signals. *J. Fluid Mech.*, 811:189–209, 2017.

[7] R. Pethiyagoda, S. W. McCue, T. J. Moroney, and J. M. Back. Jacobian-free Newton-Krylov methods with GPU acceleration for computing nonlinear ship wave patterns. *J. Comput. Phys.*, 269:297–313, 2014.

[8] R. Pethiyagoda, T. J. Moroney, G. J. Macfarlane, J. R. Binns, and S. W. McCue. Time-frequency analysis of ship wave patterns in shallow water: modelling and experiments. *Ocean Engng*, 158:123–131, 2018.

[9] A. Sheremet, U. Gravois, and M. Tian. Boat-wake statistics at Jensen Beach, Florida. *J. Waterway Port Coastal Ocean Engng*, 139:286–294, 2013.

[10] T. Torsvik, H. Herrmann, I. Didenkulova, and A. Rodin. Analysis of ship wake transformation in the coastal zone using time-frequency methods. *Proc. Est. Acad. Sci.*, 64:379–388, 2015.

[11] T. Torsvik, T. Soomere, I. Didenkulova, and A. Sheremet. Identification of ship wake structures by a time-frequency method. *J. Fluid Mech.*, 765:229–251, 2015.

[12] D. C. Wyatt and R. E. Hall. Analysis of ship-generated surface waves using a method based upon the local Fourier transform. *J. Geophys. Res. Oceans*, 93:14133–14164, 1988.